Geochemical Perspectives Letters

Running out of gas: Zircon ^{18}O-Hf-U/Pb evidence for Snowball Earth preconditioned by low degassing

J. Hartmann[1*], G. Li[2], A.J. West[3]

OPEN ACCESS

doi: 10.7185/geochemlet.1734

Abstract

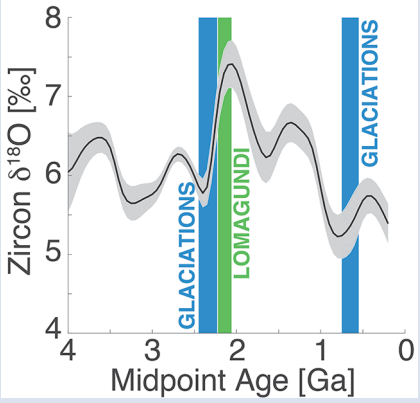

The general long-term stability of Earth's climate over geologic time was punctuated by dramatic excursions. Between *ca.* 2.5 and 0.5 billion years ago (Ga), these events included the globally extensive glaciations known as Snowball Earths, when ice extended to tropical latitudes. Such anomalous periods of time provide unique opportunities for understanding the mechanisms regulating planetary climate and habitability. However, the causes of these events remain enigmatic, in part because there is little information about fluxes in the global carbon cycle in deep time. We propose that the oxygen stable isotope composition in zircons ($\delta^{18}O_{zircon}$) contains information about past weathering conditions on the continents, imparted during the time between separation of parent material from the mantle (reflected in the Hf model age) and zircon crystallisation (the U/Pb age). A new compilation of coupled ^{18}O-Hf-U/Pb isotopic data shows that the mean $\delta^{18}O_{zircon}$ value varied particularly between 2.5 Ga and 0.5 Ga. The maximum in the $\delta^{18}O_{zircon}$ record, which we interpret as a time of intense weathering, is associated with the Lomagundi Event (~2.22–2.07 Ga), a dramatic carbon isotope excursion thought to reflect enhanced organic carbon burial facilitated by the release of phosphorous during rock weathering. The onset of the Neoproterozoic Snowball Earth events coincides with the minimum in $\delta^{18}O_{zircon}$, suggesting low silicate weathering rates at the time. This evidence suggests that long-term decreases in the rate of CO_2 release to the atmosphere from solid Earth degassing may have preconditioned the global climate system for intense glaciations.

Received 13 May 2017 | Accepted 3 August 2017 | Published 15 September 2017

Letter

Over geologic time, Earth's climate is regulated by the fluxes of carbon to and from the coupled ocean-atmosphere system, specifically by the balance between solid Earth degassing, the consumption and release of CO_2 via rock weathering, and the burial and oxidation of organic carbon (Berner, 2004). For most of Earth's history, the sources and sinks of atmospheric CO_2 have remained in close balance, maintaining the planet's equable climate (Walker *et al.*, 1983; Berner and Caldeira, 1997). The large carbon cycle anomalies observed in the sedimentary record of the Archean and Proterozoic eras represent puzzling deviations from this general stability (Hoffman *et al.*, 1998; Goddéris *et al.*, 2003; Bekker and Holland, 2012; Lyons *et al.*, 2014). Understanding the causes of these events requires information about the carbon cycle at the time, which remains scarce. Geochemical evidence from marine sediments, such as records of $^{87}Sr/^{86}Sr$ or $\delta^{13}C$, is subject to multiple interpretations (*e.g.*, Kump, 1989; Goddéris *et al.*, 2017). For example, the evolution of seawater $^{87}Sr/^{86}Sr$ over geological time (McArthur *et al.*, 2012) may be influenced by changes in degassing and hydrothermal activity, continental weatherability, and the isotopic composition of rocks undergoing weathering (Kump, 1989). Without independent constraints, marine isotopic records cannot distinguish between these possibilities, each with different implications for the carbon cycle.

Zircons may provide information about carbon cycle fluxes that is independent of the multiple factors affecting seawater composition. The Hf isotopic composition of a zircon reflects the time when the grain's unmixed parent material separated from the depleted mantle reservoir (Griffin *et al.*, 2002; Hawkesworth and Kemp, 2006). In contrast, the U/Pb age of a zircon records the last time the mineral experienced temperatures above the closure threshold for the Pb system (>1000 °C), and thus the crystallisation age (Mezger and Krogstad, 1997). The difference between the Hf and U/Pb ages, here termed $\Delta T_{Hf\text{-}U/Pb}$, represents the time interval during which zircon parent material could have been affected by weathering and magmatic processes (Fig. 1), leaving an imprint on $\delta^{18}O_{zircon}$ (Valley *et al.*, 2005). The contribution from even small amounts of altered crustal material can increase $\delta^{18}O_{zircon}$ values above the primary mantle signature of ~5.3 ± 0.3 ‰, because altered crust is isotopically enriched as a result of weathering by meteoric fluids (Savin and Epstein, 1970; Gregory and Taylor, 1981; Bindeman *et al.*, 2016). The extent of isotopic enrichment for a given zircon grain will depend on the amount

1. Institute for Geology, Center for Earth System Research and Sustainability (CEN), Universität Hamburg, Bundesstrasse 55, D-20146 Hamburg, Germany
2. MOE Key Laboratory of Surficial Geochemistry, Department of Earth Sciences, Nanjing University, 163 Xianlindadao, Nanjing 210023, China
3. Department of Earth Sciences, University of Southern California, 3651 Trousdale Parkway, Los Angeles, CA 90089, USA
* Corresponding author (email: geo@hattes.de)

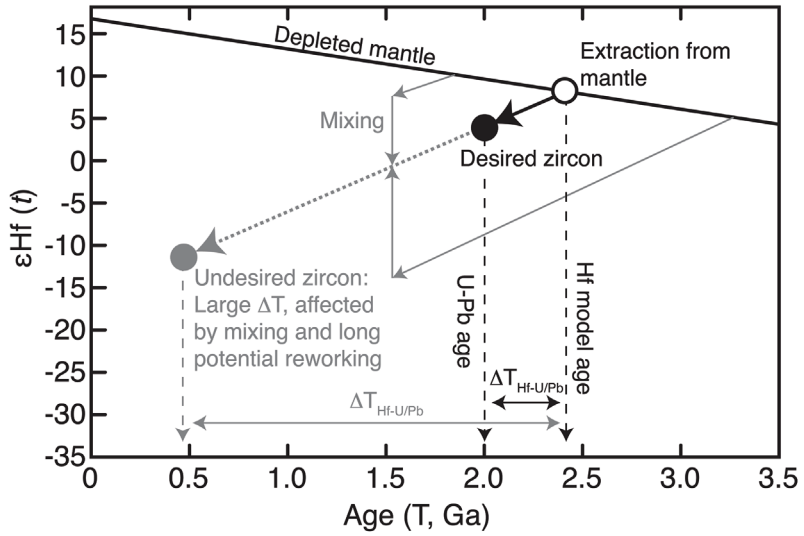

Figure 1 Schematic diagram of the age evolution of a zircon grain, showing how combined Hf and U/Pb isotope information can be used to determine the time window ($\Delta T_{Hf\text{-}U/Pb}$) during which the $\delta^{18}O_{zircon}$ value is acquired, based on the conceptual model proposed here. The Hf model age constrains the time that parent material separated from the mantle, beginning its journey of reworking *via* weathering, erosion, and incorporation into melts. This journey ends when the zircon crystallises, as represented by its U/Pb age. Longer $\Delta T_{Hf\text{-}U/Pb}$ windows may be affected by mixing and make it difficult to identify the timing when the $\delta^{18}O_{zircon}$ signature was acquired. We screen zircons by $\Delta T_{Hf\text{-}U/Pb}$ in order to calculate the time evolution of $\delta^{18}O_{zircon}$.

of weathering-related contamination of the parent magma, which is related to the alteration state of the crustal material (Valley *et al.*, 2005). More intense chemical weathering and clay formation on the continents will produce more weathered sedimentary material, with heavier $\delta^{18}O$, increasing the potential for elevating $\delta^{18}O_{zircon}$ (Valley *et al.*, 2005; Payne *et al.*, 2015; Bindeman *et al.*, 2016). Thus, a grain's $\delta^{18}O_{zircon}$ value should preserve some information about the weathering conditions during that grain's $\Delta T_{Hf\text{-}U/Pb}$ time interval. While petrologic processes and magma chamber conditions such as oxygen fugacity may also influence $\delta^{18}O_{zircon}$ by changing fractionation factors (Valley, 2003), we propose that, when averaged over grains from around the world, $\delta^{18}O_{zircon}$ reflects globally averaged weathering conditions during a given $\Delta T_{Hf\text{-}U/Pb}$ interval.

We have compiled published $\delta^{18}O$-Hf-U/Pb zircon data from predominantly detrital zircons – including in total 4444 grains with coupled information for all three isotope systems (*i.e.* all three analyses made on the same zircon crystal). These data span 4.4 Ga of Earth's history. We have calculated $\Delta T_{Hf\text{-}U/Pb}$ for each grain and evaluated the $\delta^{18}O$ of the zircons that fall within a given $\Delta T_{Hf\text{-}U/Pb}$ window. We argue that shorter windows are most likely to provide information about crustal weathering conditions during a given $\Delta T_{Hf\text{-}U/Pb}$ window. Long windows may incorporate mixing of material with different Hf-derived mantle extraction ages (Fig. 1) and also reflect the accumulated effects of reworking over long periods of time, potentially subject to long-term tectonic controls on the extent of low temperature contribution to the $\delta^{18}O$ signature. Even for short $\Delta T_{Hf\text{-}U/Pb}$, any individual zircon's $\delta^{18}O$ will be influenced by the tectonic and petrologic history of that grain's parent magma, which is likely specific to its regional origin. Thus, when plotting data from all individual grains, a very large spread is observed in $\delta^{18}O_{zircon}$ values for any given U/Pb crystallisation age (Valley *et al.*, 2005; Payne *et al.*, 2015, 2016). By aggregating many hundreds to thousands of grains from detrital sources, we seek to extract the average conditions that are most likely to represent the state of crustal alteration for defined time slices, rather than the specific history of individual zircons.

We have calculated a moving average of $\delta^{18}O_{zircon}$ over time, using a Gaussian filter. Specifically, for each time t, beginning at 4 Ga and proceeding in 50 Ma increments, we begin by calculating a weighting factor for all zircon data points. The weighting factor is determined by each zircon's age with respect to the normal distribution centred at time t, with standard deviation of 100 Ma, thus giving zircons closer to t a higher weight and effectively giving zero weight to zircons more than a few hundred million years from t. For zircon age, we average the Hf model age and the U-Pb age of each grain, to reflect the midpoint of the assumed processing time during which the grain's parent material acquired its $\delta^{18}O$ composition. We estimate a representative $\delta^{18}O_{zircon}$ value for time t by calculating a mean weighted $\delta^{18}O_{zircon}$ for all data points. The standard deviation of the mean $\delta^{18}O_{zircon}$ for time t is similarly calculated with the Gaussian weighting (±2 standard deviation shown by grey envelopes in the Figures and the Supplementary Videos).

We include only zircons that fall within a given $\Delta T_{Hf\text{-}U/Pb}$ window, while varying the size of the $\Delta T_{Hf\text{-}U/Pb}$ window from 50 Ma to 1500 Ma (see Supplementary Videos, where the number of grains considered and the mean $\Delta T_{Hf\text{-}U/Pb}$ for each time window is reported). Figure 2 shows examples, with average zircon $\delta^{18}O$ plotted *versus* time for $\Delta T_{Hf\text{-}U/Pb}$ ranging from 50 to 450 Ma. For low $\Delta T_{Hf\text{-}U/Pb}$ (<~300 Ma) the number of total data points is low (<1000 grains total), leading to larger uncertainties (Fig. 2). There is thus a tradeoff between focusing on short time windows (over which there are too few data from zircon grains to provide a conclusive picture) *versus* longer time windows (which average over longer periods of time, reducing the temporal resolution for relating to specific geologic events). For $\Delta T_{Hf\text{-}U/Pb}$ of 350–500 Ma, uncertainties are reduced and distinct patterns emerge in the data, with first order minima and maxima that remain stable across a wide range of $\Delta T_{Hf\text{-}U/Pb}$. This stability suggests these features are not artefacts of the data analysis. In the discussion that follows, we focus on the time-evolution of $\delta^{18}O_{zircon}$ calculated for grains with $\Delta T_{Hf\text{-}U/Pb} < 400$ Ma, which is representative of the first order patterns and still sufficiently short to relate to major changes in the environmental state of the Earth system. We primarily report results based on the New Crust Hf age model (Dhuime *et al.*, 2011; Payne *et al.*, 2016). For comparison, the same calculations are also presented in the Supplementary Information (Figs. S-1 and S-2) using the traditional TDM Hf model age, revealing basically the same picture.

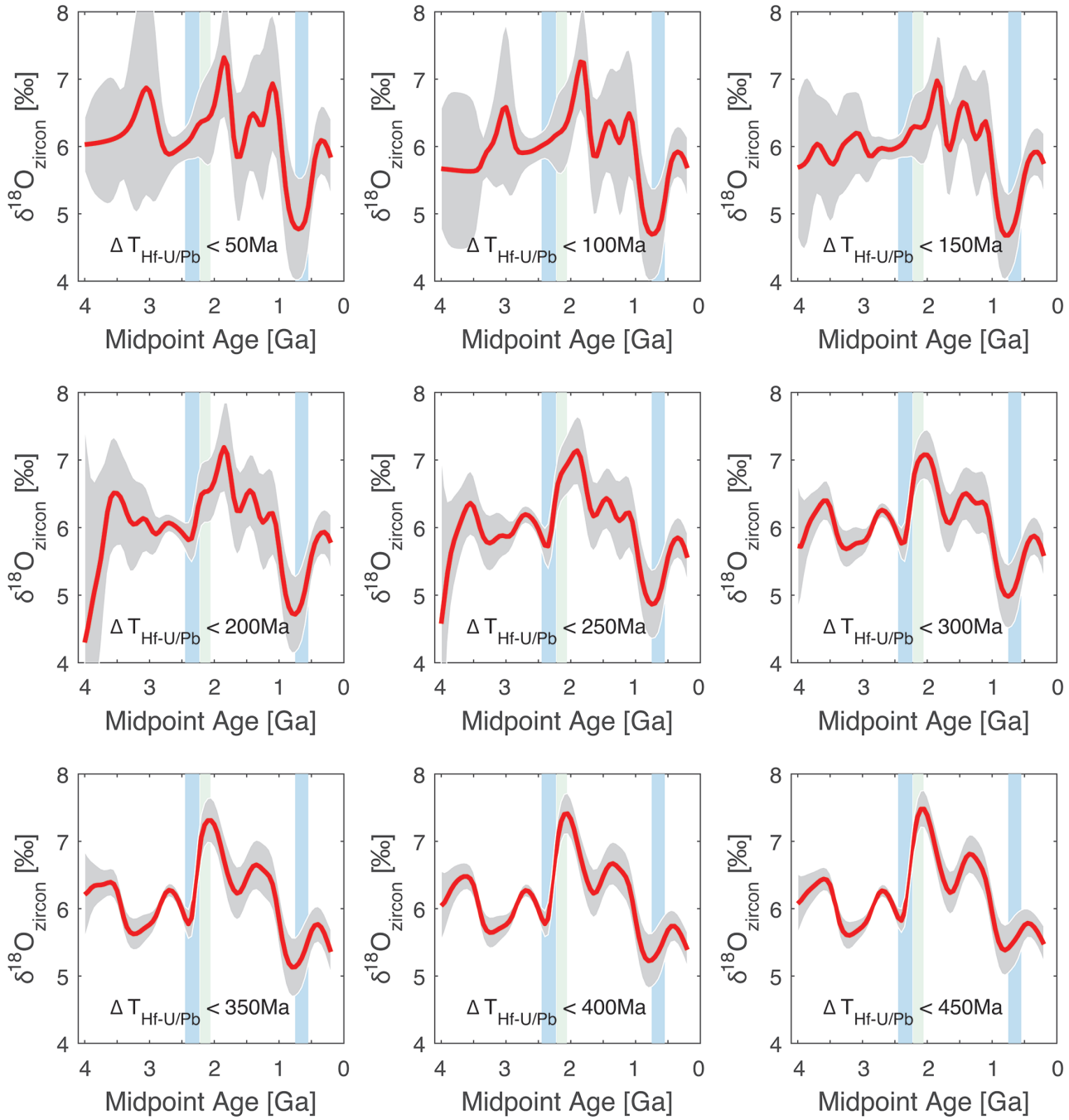

Figure 2 Time evolution of $\delta^{18}O_{zircon}$ calculated for different values of $\Delta T_{Hf\text{-}U/Pb}$ as selection criterion (see also Supplementary Video S-1). The very short values of $\Delta T_{Hf\text{-}U/Pb}$ restrict the total number of grains in the dataset to a small number (<1000 grains if $\Delta T_{Hf\text{-}U/Pb}$ <300 Ma using the New Crust Hf model age, shown here), leading to large uncertainties, although some of the first order features are still evident (*e.g.*, a maximum ~2 Ga and minimum ~0.8 Ga). For longer $\Delta T_{Hf\text{-}U/Pb}$ windows, the uncertainties are much reduced and general patterns are stable across a range of window sizes. For very large $\Delta T_{Hf\text{-}U/Pb}$ (*e.g.*, >1000 Ma; see Supplementary Video S-1) the $\delta^{18}O_{zircon}$ curve represents a long-term accumulated signal that is difficult to tie to specific geologic events because of the long integration window. The grey band represents ±2 s.d. (s.d.: standard deviation of the mean). Blue bars represent periods of glaciations in the late Archean and in the Neoproterozoic. The green bar covers the period of the Lomagundi event. Also see Figure 3.

In comparing the trends in $\delta^{18}O_{zircon}$ with the timing of geological events (Fig. 3), it is important to note that the $\delta^{18}O_{zircon}$ values aggregate effects over a time interval between the Hf model age and the U-Pb age. The timescale in Figure 3 represents average values focused at the midpoint of this interval (see above), but the weathering signature is likely to have been acquired over a longer period of time, so each time point on Figure 3 actually reflects a range of time. The size of the prescribed $\Delta T_{Hf\text{-}U/Pb}$ selection time window puts a maximum limit on this duration (in the case of Fig. 3, 400 Ma). In practice, the actual $\Delta T_{Hf\text{-}U/Pb}$ values for individual grains are often shorter than the maximum prescribed window. In the case of Figure 3, the mean $\Delta T_{Hf\text{-}U/Pb}$ is 225 Ma. This reflects the typical time over which the effects of weathering are expected to have left an imprint in the $\delta^{18}O_{zircon}$, and thus a characteristic uncertainty on the time axis of Figure 3. To facilitate comparison, this duration is illustrated by the lighter shading on the timing of geological events; this shading does not reflect uncertainty on the timing of these events themselves but rather reflects the temporal resolution of the $\delta^{18}O_{zircon}$ curve. The mean $\Delta T_{Hf\text{-}U/Pb}$ for zircons actually varies somewhat as a function of time. Supplementary Information

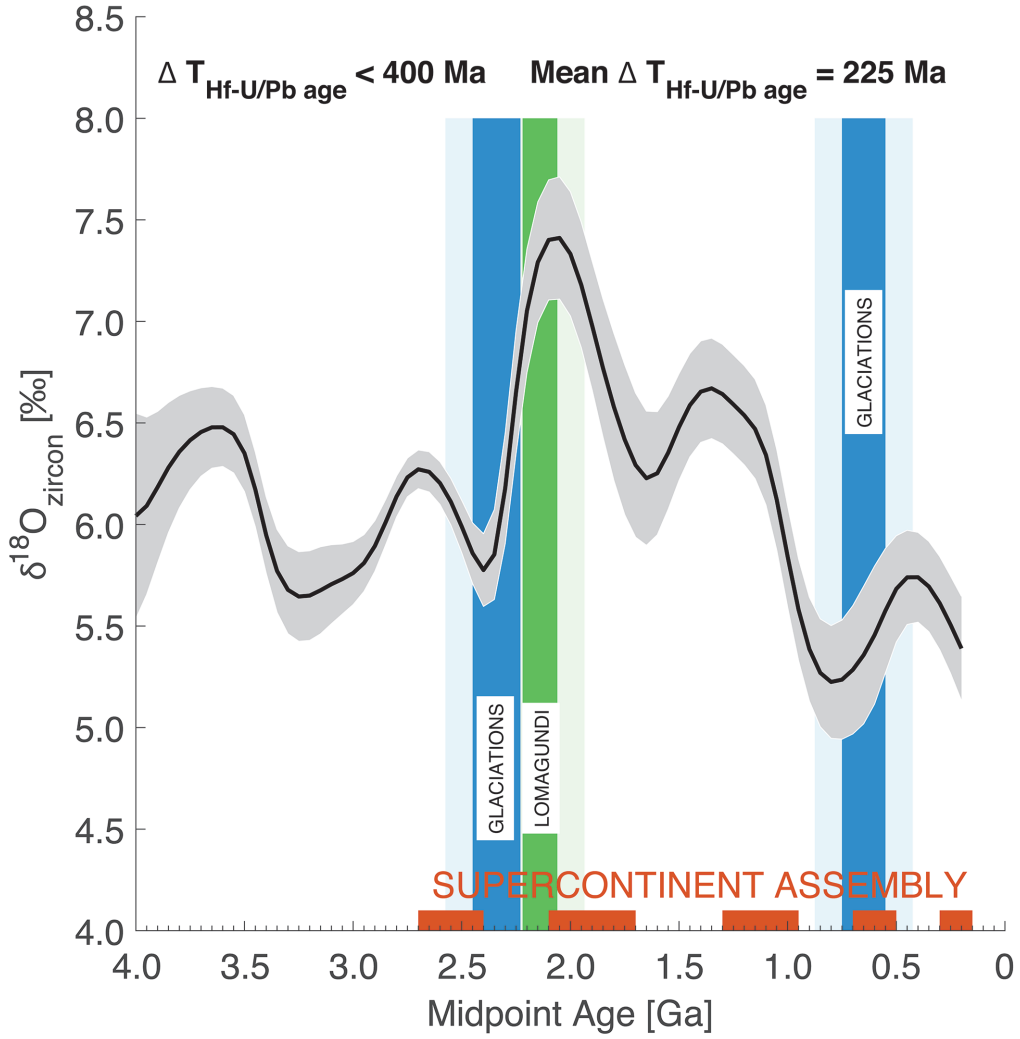

Figure 3 $\delta^{18}O_{zircon}$ calculated for $\Delta T_{Hf\text{-}U/Pb}$ <400 Ma, along with timing of major carbon cycle anomalies observed in the geologic record. The grey band represents ±2 s.d. (s.d.: standard deviation of the mean). Red bars indicate periods of supercontinent assembly (Cawood *et al.*, 2013). Dark blue bars represent periods of glaciations in the late Archean and in the Neoproterozoic. The dark green bar covers the period of the Lomagundi event. Note that the $\delta^{18}O_{zircon}$ values are plotted using the midpoint age of the $\Delta T_{Hf\text{-}U/Pb}$ window, but the actual $\delta^{18}O_{zircon}$ values integrate processes (*e.g.*, weathering conditions) occurring over longer periods of time, characterised by a mean $\Delta T_{Hf\text{-}U/Pb}$ duration of 225 Ma. To illustrate the effect on the comparison between the timing of geological events and the $\delta^{18}O_{zircon}$ curve, lighter shaded areas around periods of geological events reflect uncertainty of the $\delta^{18}O_{zircon}$ curve associated with plotting the curve for the midpoint between the Hf and U/Pb ages, given as half of the mean $\Delta T_{Hf\text{-}U/Pb}$ (112.5 Ma).

Figure S-3 shows $\delta^{18}O_{zircon}$ curves accounting for this variability by calculating the weighted standard deviation of the age at each time t. As expected, the variance in age (2 standard deviation) is ~0.1–0.2 Ga and is similar over the 4 Ga record, indicating that the single average value of 225 Ma in Figure 3, while a simplification, captures the characteristic uncertainty in the time dimension.

In common with prior studies, we see relatively little variability in $\delta^{18}O_{zircon}$ until ~2.5 Ga, considering the patterns of long-term evolution over 4 Ga (Valley *et al.*, 2005; Payne *et al.*, 2015). After 2.5 Ga, we observe that the minimum and maximum in the $\delta^{18}O_{zircon}$ record coincide with two of the most pronounced carbon cycle perturbations in the geologic record. Specifically, the rise towards the highest $\delta^{18}O_{zircon}$ in the record coincides with the Lomagundi carbon isotope excursion (*ca.* 2.22–2.07 Ga) (Bekker and Holland, 2012), while the lowest $\delta^{18}O_{zircon}$ in the record corresponds to the Neoproterozoic Snowball Earth events and the framing Kaigas, Gaskiers, and Vingerbreek glaciations (*ca.* 0.75–0.55 Ga) (Germs and Gaucher, 2012; Hofmann *et al.*, 2015). Moreover, the Archean global glaciations (*ca.* 2.45–2.24 Ga) (Gumsley *et al.*, 2017) also coincide with a local minimum in $\delta^{18}O_{zircon}$. Periods of supercontinent assembly (Cawood *et al.*, 2013) appear to occur at similar times to peaks in $\delta^{18}O_{zircon}$ (Fig. 3) and mature supercontinents with periods of lower $\delta^{18}O_{zircon}$, except during Gondwana-Pangea formation and breakup of the last 0.7 Ga.

The Lomagundi carbon isotope excursion (Karhu and Holland, 1996; Bekker and Holland, 2012; Lyons *et al.*, 2014) occurs as $\delta^{18}O_{zircon}$ rises towards the highest values in the geological record (Fig. 3), suggesting the possibility of intense weathering at the time. High weathering intensity may have resulted from high mantle degassing due to vigorous convection (Condie *et al.*, 2001, 2016; Grenholm and Scherstén, 2015), or to the onset of oxidative weathering following the rise of atmospheric O_2 (Bekker and Holland, 2012; Planavsky *et al.*, 2012). Abundant Al-rich shales and quartz-rich sandstones at the time have been cited as evidence for intense weathering conditions (Bekker, 2014), and the extremely enriched $\delta^{13}C$ values in carbonates have been explained by large amounts of organic carbon burial, resulting from enhanced biological productivity facilitated by the release of phosphorous (a limiting nutrient) during rock weathering (Bekker and Holland, 2012; Harada *et al.*, 2015). The zircon record is consistent with this hypothesis, lending some confidence to interpretation of $\delta^{18}O_{zircon}$ as reflecting global weathering conditions.

The minimum in $\delta^{18}O_{zircon}$ coinciding with the beginning of the Neoproterozoic Snowball Earth events points to a decreased imprint of weathered crust in parent magmas at these times. We suggest this signal is indicative of low weathering intensity on the continents. In simplistic terms, if glaciations were caused by drawdown of atmospheric CO_2 *via* enhanced silicate weathering, as suggested in prior studies (Goddéris *et al.*, 2003; Donnadieu *et al.*, 2004; Pierrehumbert *et al.*, 2011), the opposite would be expected, namely higher weathering intensity and thus elevated $\delta^{18}O_{zircon}$ immediately preceding and during glaciation. Global weathering fluxes should balance degassing fluxes over timescales >1 Ma, because of climate-dependent weathering feedbacks (*e.g.*, Berner and Caldeira, 1997). Thus, we propose that the minima in $\delta^{18}O_{zircon}$ reflect times of low solid Earth CO_2 degassing, which preconditioned the Earth system for glaciation by forcing a state of low atmospheric pCO_2. Low degassing flux has similarly been suggested as an underlying cause of icehouse climate states based on compilations of zircon abundance over the past ~0.7 Ga (McKenzie *et al.*, 2016).

The data presented here average over long periods of time (100s of millions of years to yield a sufficient number of grains in each time interval to extract a robust pattern). As a consequence, the results do not preclude an immediate triggering of glaciation by changes in weathering fluxes and CO_2 drawdown, for example by enhanced weathering of continental crust, large igneous provinces, or submarine basalt (Goddéris *et al.*, 2003; Donnadieu *et al.*, 2004; Gernon *et al.*, 2016). Relatively low background levels of atmospheric pCO_2, resulting from low degassing fluxes, could have set up the system for the onset of Snowball Earth, which then occurred as an immediate result of enhanced weathering events without requiring anomalously intense weathering, since pCO_2 can be more easily reduced to the levels required for runaway glaciation when the background concentrations are low. Thus, we suggest that enhanced weathering, as may have occurred during supercontinent breakup, might have been the immediate trigger, but that a long-term trajectory of low degassing set the stage for globally extensive glaciation.

The subsequent increase in $\delta^{18}O_{zircon}$ as glaciations continued (*i.e.* leading up to 0.5 Ga) might have been influenced, at least in part, by intense weathering after glaciations (*e.g.*, Hoffman *et al.*, 1998) and submarine basalt weathering (Gernon *et al.*, 2016).

Whether similar conditions prevailed at the time of the earlier Archean glaciations remains unclear from the zircon data (*e.g.*, see suggested mechanisms for the onset of Palaeoproterozoic glaciations; Teitler *et al.*, 2014), and we emphasise that the long integration window of the zircon data preclude interpretation of trends in Figure 3 in terms of individual episodes of glaciation such as specific Snowball Earth events.

Elevated values of $\delta^{18}O_{zircon}$ at times of supercontinent assembly (*i.e.* immediately preceding the red bars in Fig. 3) may be related to tectonically enhanced exchange of sediments with magma reservoirs (Spencer *et al.*, 2014). Incorporation of sediments into melts can occur within a 100 Ma time window (Payne *et al.*, 2015), short enough for the signal to propagate into the zircon record. The zircon record at times of continental assembly may also reflect increased degassing during collision (Bickle, 1996; Kerrick and Caldeira, 1998), generating high weathering fluxes and thus more altered crustal material.

As each supercontinent matured, solid Earth degassing rates and sediment exchange may have diminished, decreasing $\delta^{18}O_{zircon}$ values. More broadly, we speculate that the overall peak in $\delta^{18}O_{zircon}$ around 2 Ga and the decrease towards the present day may be attributed to diminished overall mid-ocean ridge mantle degassing rates with time due to depletion of carbon in the mantle reservoir undergoing degassing (Hofmann, 1988), if little subducted carbon is recycled into the convecting mantle (Kelemen and Manning, 2015).

In summary, based on the 4444 coupled $\delta^{18}O$-Hf-U/Pb data compiled in this study, we have identified peaks and valleys in the $\delta^{18}O_{zircon}$ record, particularly between 2.5 and 0.5 Ga, that can be pinned to <250 Ma time intervals on the basis of $\Delta T_{Hf\text{-}U/Pb}$. We suggest that changes in continental weathering can explain these observed variations in a manner that is mechanistically consistent with the alteration of crustal material leaving a characteristic isotopic signature in zircon parent material. Inferred changes in continental weathering over time help to explain first order geologic events including the Neoproterozoic Snowball Earth episodes, which we argue based on the zircon record were preconditioned by low solid Earth degassing over the long-term. More rigorous testing of these hypothesised relationships will require better understanding of the links between increases in $\delta^{18}O_{zircon}$, the propagation of altered crust isotopic signature into parent magmas, and global continental weathering conditions.

Additional data collection and analysis, for example at higher temporal resolution, could help to refine understanding of relationships between $\delta^{18}O_{zircon}$ and weathering conditions, including identifying the optimal $\Delta T_{Hf\text{-}U/Pb}$ that captures the effect of geological events on the $\delta^{18}O_{zircon}$ signal.

It might be possible to scale $\delta^{18}O_{zircon}$ with changes in mantle degassing rate, given sufficient information about fractionation during weathering and incorporation of this signal into crustal melts, opening the possibility of extending the evaluations considered in this study to semi-quantitative interpretations. But with present constraints, the proxy remains qualitative, and indeed many factors other than continental weathering are likely to influence the $\delta^{18}O$ of zircons. Nonetheless, even without a further leap of quantitatively linking $\delta^{18}O_{zircon}$ to carbon fluxes, we propose that coupled $\delta^{18}O$-Hf-U/Pb data from zircons have the promise to illuminate links between mantle dynamics, plate tectonics, and weathering processes, helping to unravel the processes regulating Earth's carbon cycle and climate over geologic time.

Acknowledgements

This work was supported by the German Science Foundation DFG (Cluster of Excellence 'CliSAP', EXC177, Universität Hamburg), the National Natural Science Foundation of China (grant nos. 41422205 and 41730101), and the US National Science Foundation (grant no. 1338329). The authors thank Wagner de Oliveira Garcia and Thorben Amann for help copying the data and making the videos. T.M. Gernon and one anonymous reviewer are thanked for constructive comments, and E. Oelkers for editorial handling.

Editor: Eric Oelkers

Author contributions

J.H. and G.L. designed the study. J.H. collected the data. J.H., G.L., A.J.W. conducted the research and wrote the manuscript.

Additional Information

Supplementary Information accompanies this letter at www.geochemicalperspectivesletters.org/article1734

Cite this letter as: Hartmann, J., Li, G., West, A.J. (2017) Running out of gas: Zircon ^{18}O-Hf-U/Pb evidence for Snowball Earth preconditioned by low degassing. *Geochem. Persp. Let.* 4, 41–46.

References

Bekker, A. (2014) Lomagundi Carbon Isotope Excursion. In: Amils, R., Gargaud, M., Cernicharo Quintalla, J., Cleaves, H.J., Irvine, W.M., Pinti, D., Viso, M. (Eds.) Encyclopedia of Astrobiology. Springer, Berlin, Heidelberg, 1–6.

Bekker, A., Holland, H.D. (2012) Oxygen overshoot and recovery during the early Paleoproterozoic. *Earth and Planetary Science Letters* 317–318, 295–304.

Berner, R.A. (2004) *The Phanerozoic Carbon Cycle: CO2 and O2*. Oxford University Press, New York.

Berner, R.A., Caldeira, K. (1997) The need for mass balance and feedback in the geochemical carbon cycle. *Geology* 25, 955–956.

Bickle, M.J. (1996) Metamorphic decarbonation, silicate weathering and the long-term carbon cycle. *Terra Nova* 8, 270–276.

Bindeman, I.N., Bekker, A., Zakharov, D.O. (2016) Oxygen isotope perspective on crustal evolution on early Earth: A record of Precambrian shales with emphasis on Paleoproterozoic glaciations and Great Oxygenation Event. *Earth and Planetary Science Letters* 437, 101–113.

Cawood, P.A., Hawkesworth, C.J., Dhuime, B. (2013) The continental record and the generation of continental crust. *GSA Bulletin* 125, 14–32.

Condie, K.C., Aster, R.C., van Hunen, J. (2016) A great thermal divergence in the mantle beginning 2.5 Ga: Geochemical constraints from greenstone basalts and komatiites. *Geoscience Frontiers* 7, 543–553.

Condie, K.C., Des Marais, D.J., Abbott, D. (2001) Precambrian superplumes and supercontinents: a record in black shales, carbon isotopes, and paleoclimates? *Precambrian Research* 106, 239–260.

Dhuime, B., Hawkesworth, C., Cawood, P. (2011) When continents formed. *Science* 331, 154–155.

Donnadieu, Y., Goddéris, Y., Ramstein, G., Nédélec, A., Meert, J. (2004) A 'snowball Earth' climate triggered by continental break-up through changes in runoff. *Nature* 428, 303–306.

Germs, G.J.B., Gaucher, C. (2012) Nature and extent of a late Ediacaran (ca. 547 Ma) glacigenic erosion surface in southern Africa. *South African Journal of Geology* 115, 91–102.

Gernon, T.M., Hincks, T.K., Tyrrell, T., Rohling, E.J., Palmer, M.R. (2016) Snowball Earth ocean chemistry driven by extensive ridge volcanism during Rodinia breakup. *Nature Geoscience* 9, 242–248.

Goddéris, Y., Donnadieu, Y., Nédélec, A., Dupré, B., Dessert, C., Grard, A., Ramstein, G., François, L.M. (2003) The Sturtian 'snowball' glaciation: fire and ice. *Earth and Planetary Science Letters* 211, 1–12.

Goddéris, Y., Le Hir, G., Macouin, M., Donnadieu, Y., Hubert-Théou, L., Dera, G., Aretz, M., Fluteau, F., Li, Z.X., Halverson, G.P. (2017) Paleogeographic forcing of the strontium isotopic cycle in the Neoproterozoic. *Gondwana Research* 42, 151–162.

Gregory, R.T., Taylor, H.P. (1981) An oxygen isotope profile in a section of Cretaceous oceanic crust, Samail Ophiolite, Oman: Evidence for δ18O buffering of the oceans by deep (> 5 km) seawater-hydrothermal circulation at mid-ocean ridges. *Journal of Geophysical Research: Solid Earth* 86, 2737–2755.

Grenholm, M., Scherstén, A. (2015) A hypothesis for Proterozoic-Phanerozoic supercontinent cyclicity, with implications for mantle convection, plate tectonics and Earth system evolution. *Tectonophysics* 662, 434–453.

Griffin, W.L., Wang, X., Jackson, S.E., Pearson, N.J., O'Reilly, S.Y., Xu, X., Zhou, X. (2002) Zircon chemistry and magma mixing, SE China: in-situ analysis of Hf isotopes, Tonglu and Pingtan igneous complexes. *Lithos* 61, 237–269.

Gumsley, A.P., Chamberlain, K.R., Bleeker, W., Soderlund, U., de Kock, M.O., Larsson, E.R., Bekker, A. (2017) Timing and tempo of the Great Oxidation Event. *Proc Natl Acad Sci U S A* 114, 1811–1816.

Harada, M., Tajika, E., Sekine, Y. (2015) Transition to an oxygen-rich atmosphere with an extensive overshoot triggered by the Paleoproterozoic snowball Earth. *Earth and Planetary Science Letters* 419, 178–186.

Hawkesworth, C.J., Kemp, A.I.S. (2006) Using hafnium and oxygen isotopes in zircons to unravel the record of crustal evolution. *Chemical Geology* 226, 144–162.

Hoffman, P.F., Kaufman, A.J., Halverson, G.P., Schrag, D.P. (1998) A Neoproterozoic snowball earth. *Science* 281, 1342–1346.

Hofmann, A.W. (1988) Chemical differentiation of the Earth: the relationship between mantle, continental crust, and oceanic crust. *Earth and Planetary Science Letters* 90, 297–314.

Hofmann, M., Linnemann, U., Hoffmann, K.-H., Germs, G., Gerdes, A., Marko, L., Eckelmann, K., Gärtner, A., Krause, R. (2015) The four Neoproterozoic glaciations of southern Namibia and their detrital zircon record: The fingerprints of four crustal growth events during two supercontinent cycles. *Precambrian Research* 259, 176–188.

Karhu, J.A., Holland, H.D. (1996) Carbon isotopes and the rise of atmospheric oxygen. *Geology* 24, 867–870.

Kelemen, P.B., Manning, C.E. (2015) Reevaluating carbon fluxes in subduction zones, what goes down, mostly comes up. *Proceedings of the National Academy of Science of the USA* 112, E3997–4006.

Kerrick, D.M., Caldeira, K. (1998) Metamorphic CO2 degassing from orogenic belts. *Chemical Geology* 145, 213–232.

Kump, L.R. (1989) Alternative modeling approaches to the geochemical cycles of carbon, sulfur, and strontium isotopes. *American Journal of Science* 289, 390–410.

Lyons, T.W., Reinhard, C.T., Planavsky, N.J. (2014) The rise of oxygen in Earth's early ocean and atmosphere. *Nature* 506, 307–315.

McArthur, J.M., Howarth, R.J., Shields, G.A. (2012) Sr isotope time series. In: Gradstein, F., Ogg, J., Schmitz, M., Ogg, G. (Eds.) *The Geological Timescale 2012*. Elsevier, Oxford, Amsterdam, Waltham, 127–144.

McKenzie, N.R., Horton, B.K., Loomis, S.E., Stockli, D.F., Planavsky, N.J., Lee, C.-T.A. (2016) Continental arc volcanism as the principal driver of icehouse-greenhouse variability. *Science* 352, 444–447.

Mezger, K., Krogstad, E.J. (1997) Interpretation of discordant U-Pb zircon ages: An evaluation. *Journal of Metamorphic Geology* 15, 127–140.

Payne, J.L., Hand, M., Pearson, N.J., Barovich, K.M., McInerney, D.J. (2015) Crustal thickening and clay: Controls on O isotope variation in global magmatism and siliciclastic sedimentary rocks. *Earth and Planetary Science Letters* 412, 70–76.

Payne, J.L., McInerney, D.J., Barovich, K.M., Kirkland, C.L., Pearson, N.J., Hand, M. (2016) Strengths and limitations of zircon Lu-Hf and O isotopes in modelling crustal growth. *Lithos* 248–251, 175–192.

Pierrehumbert, R.T., Abbot, D.S., Voigt, A., Koll, D. (2011) Climate of the Neoproterozoic. *Annual Review of Earth and Planetary Sciences* 39, 417–460.

Planavsky, N.J., Bekker, A., Hofmann, A., Owens, J.D., Lyons, T.W. (2012) Sulfur record of rising and falling marine oxygen and sulfate levels during the Lomagundi event. *Proceedings of the National Academy of Sciences* 109, 18300–18305.

Savin, S.M., Epstein, S. (1970) The oxygen and hydrogen isotope geochemistry of clay minerals. *Geochimica et Cosmochimica Acta* 84, 25–42.

Spencer, C. J., Cawood, P.A., Hawkesworth, C.J., Raub, T.D., Prave, A.R., Roberts, N.M.W. (2014) Proterozoic onset of crustal reworking and collisional tectonics: Reappraisal of the zircon oxygen isotope record. *Geology* 42, 451–454.

Teitler, Y., Le Hir, G., Fluteau, F., Philippot, P., Donnadieu, Y. (2014) Investigating the Paleoproterozoic glaciations with 3-D climate modeling. *Earth and Planetary Science Letters* 395, 71–80.

Valley, J.W. (2003) Oxygen isotopes in zircon. *Reviews in Mineralogy and Geochemistry* 53, 343–385.

Valley, J.W., Lackey, J.S., Cavosie, A.J., Clechenko, C.C., Spicuzza, M.J., Basei, M.A.S., Bindeman, I.N., Ferreira, V.P., Sial, A.N., King, E.M., Peck, W.H., Sinha, A.K., Wei, C.S. (2005) 4.4 billion years of crustal maturation: oxygen isotope ratios of magmatic zircon. *Contributions to Mineralogy and Petrology* 150, 561–580.

Walker, J.C.G., Klein, C., Schidlowski, M., Schopf, J.W., Stevenson, D.J., Walter, M.R. (1983) Environmental evolution of the Archean-early Proterozoic Earth. In: Schopf, J.W. (Ed.) *Earth's earliest biosphere: Its origin and evolution (A84-43051 21-51)*. Princeton University Press, Princeton, New Jersey, 260–290.

Geochemical Perspectives Letters

Running out of gas: Zircon ^{18}O-Hf-U/Pb evidence for Snowball Earth preconditioned by low degassing

J. Hartmann[1*], G. Li[2], A.J. West[3]

Supplementary Information

The Supplementary Information includes:

- Selection of Data
- Differences in the Hf Model Age Calculations
- Videos S-1 and S-2 (available online only)
- Figures S-1 to S-3
- Tables S-1 and S-2
- Supplementary Information References

Selection of Data

In addition to a previously published compilation of coupled $\delta^{18}O$-Hf-U-Pb data from zircons (Dhuime *et al.*, 2012), data were compiled from 18 other literature sources reporting detrital zircon analyses (Table S-1). Data were included for zircons with values for $\delta^{18}O$, U/Pb-age, and Lu and Hf isotopes measurements all on the same grain, with the latter allowing calculation of Hf model ages. Datasets were copied from supplementary source files of the given publications or from tables provided in the publications.

In most cases, U/Pb age was reported in the source publication, though in some cases ages were not reported and were calculated based on published isotope ratios. In latter cases, data were restricted to results showing discordance less than 10 % for the $^{207}Pb/^{206}Pb$, $^{206}Pb/^{238}U$ and $^{207}Pb/^{235}U$ age.

$^{176}Lu/^{177}Lu$ and $^{176}Hf/^{177}Hf$ isotope ratios were used to calculate the New Crust and the TDM Hf-model ages following the approach and data provided by Payne *et al.* (2016), with $\lambda = 1.865\ 10^{-11}\ a^{-1}$ (the decay constant for ^{176}Lu), $^{176}Hf/^{177}Hf = 0.283251$ for the CHUR-like composition, and $^{176}Lu^{0}/^{177}\ Hf_{DM} = 0.0384$ for the today's depleted mantle (DM is depleted mantle). The New Crust and TDM Hf model ages were newly calculated with these parameters for all compiled data, using the published isotope ratios.

In 22 and 92 cases, the difference between the Hf model ages (traditional TDM and New Crust, respectively) and the U/Pb-age was negative and set to zero. Reported rim-data from Zeh *et al.* (2014) were removed.

Table S-1 New data sources with coupled $\delta^{18}O$, U/Pb age and Hf model age information in addition to Dhuime *et al.* (2012).

Source Reference	Number of data points
Canile *et al.* (2016)	170
Castillo *et al.* (2016)	167
Davis *et al.* (2015)	128
Ge *et al.* (2014)	37
Herve *et al.* (2013)	149
Hollis *et al.* (2014)	184
Iizuka *et al.* (2013)	442
Jiang *et al.* (2015)	158
Li *et al.* (2012)	257
Meinhold *et al.* (2014)	29
Pankhurst *et al.* (2016)	161
Partin *et al.* (2014)	130
Wang *et al.* (2012)	125
Yang *et al.* (2015)	324
Yin *et al.* (2012)	131
Zeh *et al.* (2014)	132
Zhang *et al.* (2016)	143
Zhang *et al.* (2014)	201
Count new sources	**3068**
Dhuime *et al.* (2012)	1376
Sum of all used data points	**4444**

1. Institute for Geology, Center for Earth System Research and Sustainability (CEN), Universität Hamburg, Bundesstrasse 55, D-20146 Hamburg, Germany
2. MOE Key Laboratory of Surficial Geochemistry, Department of Earth Sciences, Nanjing University, 163 Xianlindadao, Nanjing 210023, China
3. Department of Earth Sciences, University of Southern California, 3651 Trousdale Parkway, Los Angeles, CA 90089, USA
* Corresponding author (email: geo@hattes.de)

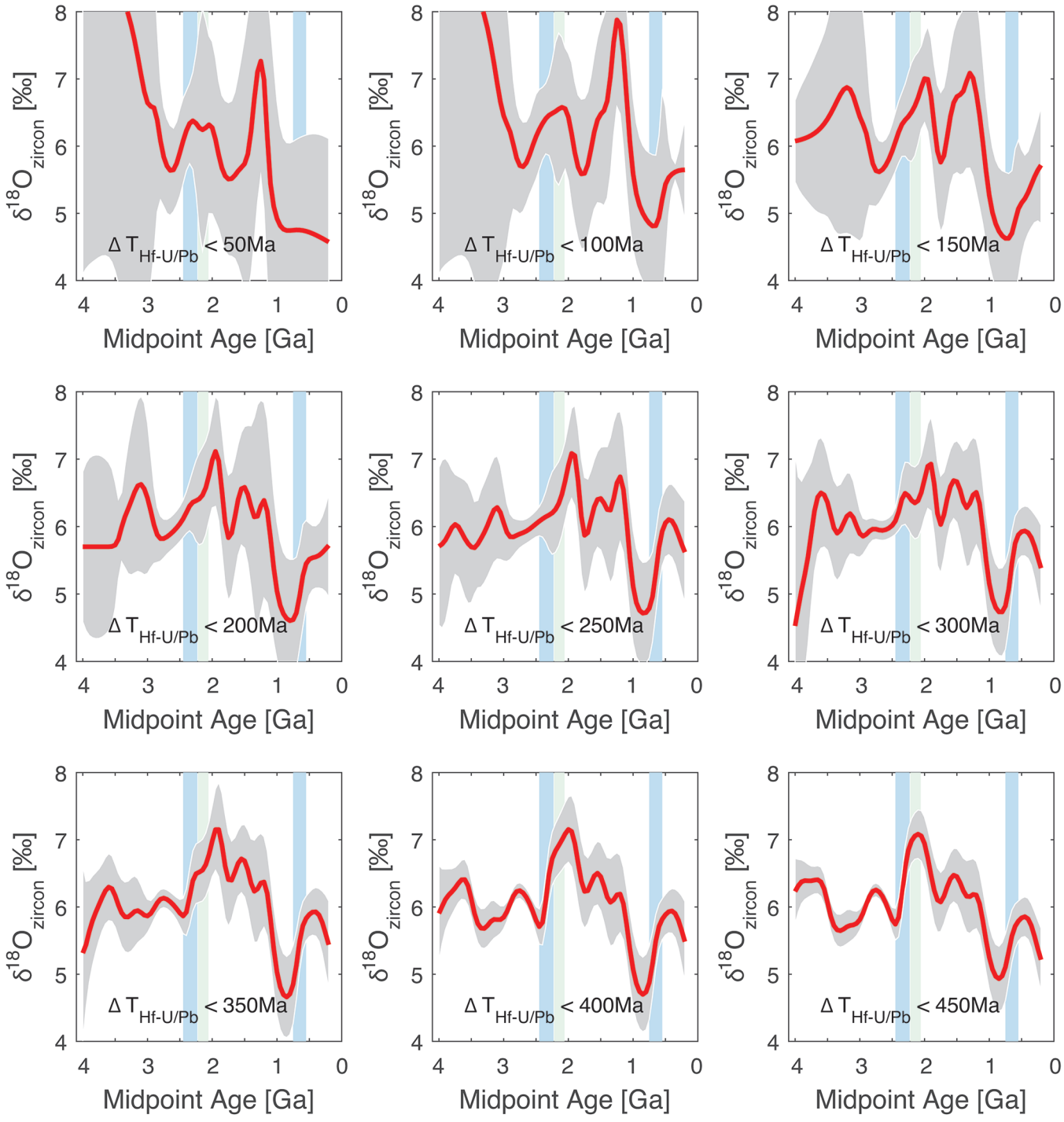

Figure S-1 Results as in Figure 2 in the main text, but using the traditional TDM Hf model age instead of the New Crust Hf model age. Time evolution of $\delta^{18}O_{zircon}$ calculated for different values of $\Delta T_{Hf\text{-}U/Pb}$ as selection criterion (see also Supplementary Video S-2). The very short values of the selection criterion $\Delta T_{Hf\text{-}U/Pb}$ restrict the total number of grains in the dataset to a small number (<400 grains if $\Delta T_{Hf\text{-}U/Pb}$ <300 Ma and using the TDM Hf model age). Blue bars represent periods of glaciations in the late Archean and in the Neoproterozoic. The green bar covers the period of the Lomagundi event.

Differences in the Hf Model Age Calculations

The differences between the TDM and New Crust Hf model ages result in slightly younger ages, of on average 150 Ma, for the New Crust Hf model ages. The location of discussed minima and maxima in the time series therefore shift slightly. The main conclusions if comparing results applying both Hf model age types do not change, *i.e.* the minima and maxima as discussed in the main text are still within the time window of relevance for given geological events. Results based on the traditional TDM Hf model age calculation are shown in Figures S-1 and S-2.

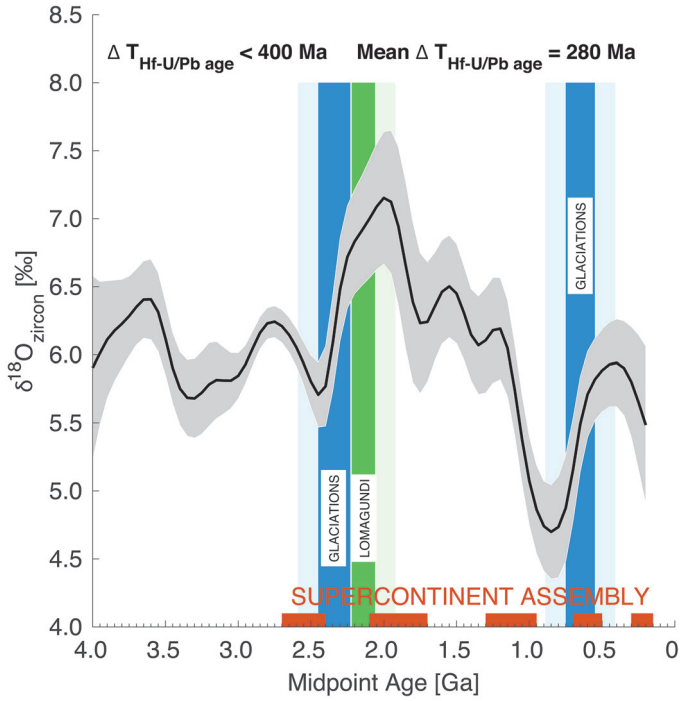

Figure S-2 Results as in Figure 3 in the main text, but using the traditional TDM Hf model age instead of the New Crust Hf model age. Note that, due the difference in the calculation procedure, the New Crust Hf model age for single grains provides on average 150 Ma shorter ages than the TDM Hf model age. Dark blue bars represent periods of glaciations in the late Archean and in the Neoproterozoic. The dark green bar covers the period of the Lomagundi event. To illustrate the effect on comparison between the timing of geological events and the $\delta^{18}O_{zircon}$ curve, lighter shaded areas around periods of geological events reflect uncertainty of the $\delta^{18}O_{zircon}$ curve associated with plotting the curve for the midpoint between the Hf and U/Pb ages, given as half of the mean $\Delta T_{Hf\text{-}U/Pb}$ (140 Ma).

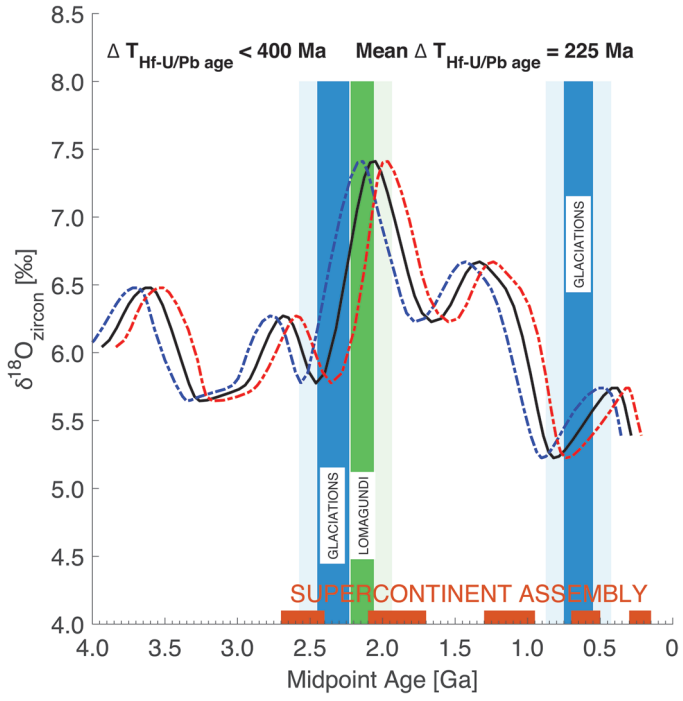

Figure S-3 Results as in Figure 3 in the main text, but with analysis of variance in ages for the population of zircons with $\Delta T_{Hf\text{-}U/Pb}$ <400 Ma. The black line shows $\delta^{18}O_{zircon}$ using the weighted mean zircon age of the selected data, when age is weighted using the same Gaussian filtering procedure as applied to the $\delta^{18}O_{zircon}$ data in Figure 3 in the main text. As expected, the weighted age (black line) plots very similarly to the actual ages used in Figure 3. The dashed blue and red lines show $\delta^{18}O_{zircon}$ plotted against time considering variance in the ages of the zircon population, specifically the weighted ±1 standard deviation of the age using the same Gaussian filtering as applied to the $\delta^{18}O_{zircon}$ data for the midpoint ages (blue: minus 1 s.d.; red: plus 1 s.d.). Weighted variance in ages ranges from 66 to 130 Ma and does not change systematically over time, so we consider the single average value reported in the text (225 Ma) as representative of the time resolution of the record for a $\Delta T_{Hf\text{-}U/Pb}$ window <400 Ma.

Supplementary Videos

The supplementary videos (available in the online version of this letter at http://www.geochemicalperspectivesletters.org/article1734) show the evolution of the $\delta^{18}O$ time series with increasing $\Delta T_{Hf\text{-}U/Pb}$ time window as selection filter for both approaches to calculate the Hf-model age. The videos also provide for each time step the number of included data points and the mean $\Delta T_{Hf\text{-}U/Pb}$ for data points fulfilling the selection criterion.

Video S-1 This supplementary video shows the evolution of the $\delta^{18}O$ time series with increasing $\Delta T_{Hf\text{-}U/Pb}$ time window as selection filter for the New Crust Hf model age. The video also provides for each time step the number of included data points and the mean $\Delta T_{Hf\text{-}U/Pb}$ for data points fulfilling the selection criterion.

Video S-2 This supplementary video shows the evolution of the $\delta^{18}O$ time series with increasing $\Delta T_{Hf\text{-}U/Pb}$ time window as selection filter for the traditional TDM Hf model age. The video also provides for each time step the number of included data points and the mean $\Delta T_{Hf\text{-}U/Pb}$ for data points fulfilling the selection criterion.

Supplementary Data Table

Table S-2 is available for download at http://www.geochemicalperspectivesletters.org/article1734.

Table S-2 Applied data including $\delta^{18}O$, hafnium and lutetium isotopic data, the uranium-lead-isotope age and references. **(a)** New compiled data. **(b)** Dhuime *et al.* (2012) data.

Supplementary Information References

Canile, F.M., Babinski, M., Rocha-Campos, A.C. (2016) Evolution of the Carboniferous-Early Cretaceous units of Paraná Basin from provenance studies based on U-Pb, Hf and O isotopes from detrital zircons. *Gondwana Research* 40, 142–169.

Castillo, P., Fanning, C.M., Hervé, F., Lacassie, J.P. (2016) Characterisation and tracing of Permian magmatism in the south-western segment of the Gondwanan margin; U–Pb age, Lu–Hf and O isotopic compositions of detrital zircons from metasedimentary complexes of northern Antarctic Peninsula and western Patagonia. *Gondwana Research* 36, 1–13.

Davis, W.J., Ootes, L., Newton, L., Jackson, V., Stern, R.A. (2015) Characterization of the Paleoproterozoic Hottah terrane, Wopmay Orogen using multi-isotopic (U-Pb, Hf and O) detrital zircon analyses: An evaluation of linkages to northwest Laurentian Paleoproterozoic domains. *Precambrian Research* 269, 296–310.

Dhuime, B., Hawkesworth, C.J., Cawood, P.A., Storey, C.D. (2012) A Change in the Geodynamics of Continental Growth 3 Billion Years Ago. *Science* 335, 1334–1336.

Ge, R., Zhu, W., Wilde, S.A., He, J. (2014) Zircon U–Pb–Lu–Hf–O isotopic evidence for ≥3.5Ga crustal growth, reworking and differentiation in the northern Tarim Craton. *Precambrian Research* 249, 115–128.

Hervé, F., Calderón, M., Fanning, C.M., Pankhurst, R.J., Godoy, E. (2013) Provenance variations in the Late Paleozoic accretionary complex of central Chile as indicated by detrital zircons. *Gondwana Research* 23, 1122–1135.

Hollis, J.A., Carson, C.J., Glass, L.M., Kositcin, N., Scherstén, A., Worden, K.E., Armstrong, R.A., Yaxley, G.M., Kemp, A.I.S. (2014) Detrital zircon U–Pb–Hf and O isotope character of the Cahill Formation and Nourlangie Schist, Pine Creek Orogen: Implications for the tectonic correlation and evolution of the North Australian Craton. *Precambrian Research* 246, 35–53.

Iizuka, T., Campbell, I.H., Allen, C.M., Gill, J.B., Maruyama, S., Makoka, F. (2013) Evolution of the African continental crust as recorded by U–Pb, Lu–Hf and O isotopes in detrital zircons from modern rivers. *Geochimica et Cosmochimica Acta* 107, 96–120.

Jiang, X.-Y., Li, X.-H., Collins, W.J., Huang, H.-Q. (2015) U-Pb age and Hf-O isotopes of detrital zircons from Hainan Island: Implications for Mesozoic subduction models. *Lithos* 239, 60–70.

Li, X.-H., Li, Z.-X., He, B., Li, W.-X., Li, Q.-L., Gao, Y., Wang, X.-C. (2012) The Early Permian active continental margin and crustal growth of the Cathaysia Block: In situ U–Pb, Lu–Hf and O isotope analyses of detrital zircons. *Chemical Geology* 328, 195–207.

Meinhold, G., Morton, A.C., Fanning, C.M., Howard, J.P., Phillips, R.J., Strogen, D., Whitham, A.G. (2014) Insights into crust formation and recycling in North Africa from combined U–Pb, Lu–Hf and O isotope data of detrital zircons from Devonian sandstone of southern Libya. *Geological Society, London, Special Publications* 386, 281–292.

Pankhurst, R.J., Hervé, F., Fanning, C.M., Calderón, M., Niemeyer, H., Griem-Klee, S., Soto, F. (2016) The pre-Mesozoic rocks of northern Chile: U–Pb ages, and Hf and O isotopes. *Earth-Science Reviews* 152, 88–105.

Partin, C.A., Bekker, A., Sylvester, P.J., Wodicka, N., Stern, R.A., Chacko, T., Heaman, L.M. (2014) Filling in the juvenile magmatic gap: Evidence for uninterrupted Paleoproterozoic plate tectonics. *Earth and Planetary Science Letters* 388, 123–133.

Payne, J.L., McInerney, D.J., Barovich, K.M., Kirkland, C.L., Pearson, N.J., Hand, M. (2016) Strengths and limitations of zircon Lu-Hf and O isotopes in modelling crustal growth. *Lithos* 248–251, 175–192.

Wang, X.-C., Li, X.-h., Li, Z.-X., Li, Q.-l., Tang, G.-Q., Gao, Y.-Y., Zhang, Q.-R., Liu, Y. (2012) Episodic Precambrian crust growth: Evidence from U–Pb ages and Hf–O isotopes of zircon in the Nanhua Basin, central South China. *Precambrian Research* 222–223, 386–403.

Yang, C., Li, X.-H., Wang, X.-C., Lan, Z. (2015) Mid-Neoproterozoic angular unconformity in the Yangtze Block revisited: Insights from detrital zircon U–Pb age and Hf–O isotopes. *Precambrian Research* 266, 165–178.

Yin, Q.Z., Wimpenny, J., Tollstrup, D.L., Mange, M., Dewey, J.F., Zhou, Q., Li, X.H., Wu, F.Y., Li, Q.L., Liu, Y., Tang, G.Q. (2012) Crustal evolution of the South Mayo Trough, western Ireland, based on U-Pb ages and Hf-O isotopes in detrital zircons. *Journal of the Geological Society* 169, 681–689.

Zeh, A., Stern, R.A., Gerdes, A. (2014) The oldest zircons of Africa—Their U–Pb–Hf–O isotope and trace element systematics, and implications for Hadean to Archean crust–mantle evolution. *Precambrian Research* 241, 203–230.

Zhang, H.-F., Wang, J.-L., Zhou, D.-W., Yang, Y.-H., Zhang, G.-W., Santosh, M., Yu, H., Zhang, J. (2014) Hadean to Neoarchean episodic crustal growth: Detrital zircon records in Paleoproterozoic quartzites from the southern North China Craton. *Precambrian Research* 254, 245–257.

Zhang, H.-F., Zhang, J., Zhang, G.-W., Santosh, M., Yu, H., Yang, Y.-H., Wang, J.-L. (2016) Detrital zircon U–Pb, Lu–Hf, and O isotopes of the Wufoshan Group: Implications for episodic crustal growth and reworking of the southern North China craton. *Precambrian Research* 273, 112–128.